Interval-Based Localization using RSSI Comparison in MANETs

FARAH MOURAD
HICHEM SNOUSSI
Université de Technologie de Troyes

CÉDRIC RICHARD
Université de Nice Sophia-Antipolis

The knowledge of node positions is essential to many applications of wireless sensor networks. We propose an original model-free technique for localization in mobile ad hoc sensor networks (MANETs). Region constraints are set by a comparison of the received signal strength indicators (RSSIs) at both anchors and nonanchor nodes. The accuracy of this method remains in the way that it overcomes the use of the channel pathloss model. It is thus naturally adapted to nonstationary environments. The proposed approach uses interval analysis and constraints satisfaction techniques to compute accurate locations in a guaranteed way. Simulations are performed on group trajectories of sensors whose movements are generated using a reference point group mobility model. The simulation results confirm the efficiency of the proposed method and show that it outperforms the anchor-based methods in terms of accuracy and estimation errors.

Manuscript received December 7, 2009; revised July 1, 2010; released for publication November 4, 2010.

IEEE Log No. T-AES/47/4/942909.

Refereeing of this contribution was handled by S. Marano.

Authors' addresses: F. Mourad and H. Snoussi, Institut Charles Delaunay (ICD)—LM2S (UMR STMR 6279), Université de Technologie de Troyes, 12, rue Marie Curie, BP 2060, 10010 Troyes cedex, France, E-mail: (farah.mourad@utt.fr); C. Richard, Laboratoire FIZEAU (UMR CNRS 6525), Université de Nice Sophia-Antipolis, Parc Valrose, 06108 Nice cedex 02, France.

I. INTRODUCTION

In recent years, mobile ad-hoc sensor networks (MANETs) have attracted great interest from researchers in the field of signal processing and wireless communications [1–3]. Such networks are composed of a large number of low-cost and densely deployed smart sensors [4]. These tiny components have processing and communication capabilities but are limited in computational capacities and memory resources. One of the most important constraints of the sensors is their low energy consumption requirement. Therefore, sensors protocols and built-in algorithms must focus primarily on energy conservation in order to extend the network lifetime.

MANETs have been broadly applied in various fields, such as military, health monitoring, and environment observation [1, 5–7]. Sensor networks have also stimulated research in information acquisition, processing and transmission in wireless devices such as mobile phones. A major advantage of MANETs is in their wireless nature as they can be deployed more rapidly and less expensively than wired networks. However, the lack of an explicit fixed infrastructure also becomes a major disadvantage in uncontrolled mobility networks due to the continuous change of sensors locations. In fact, in almost all the applications of MANETs, observed information is tightly related to the geographical locations of sensors. For this reason, the self-localization of sensors has been a primary focus of many researchers in MANETs field. The first direct way to obtain location information is to install Global Positioning Systems (GPS) on all sensors [8]. However, this solution is currently impractical as GPS receivers are expensive, high energy consuming, and relatively massive for tiny sensor devices.

Many localization algorithms have been proposed in literature to estimate sensors positions. Most of the proposed methods assume that a few number of sensors are equipped with localization hardware such as GPS receivers. These sensors, that know their positions, are called anchors. All remaining sensors are called nonanchor nodes (or simply nodes). They exchange information with anchors in order to estimate their positions. Anchor-based approaches using repetitive static localization are presented in [9], [10], [11], and [12]. For instance, in [9], each node defines its position as the center of all detected anchors within its vicinity at every time step. However, the main drawback of these methods is that they do not take advantage of the mobility of the nodes. In [13], [14], [15], techniques are proposed for data fusion or node selection aiming at targets localization. In these methods, the location estimation is performed outside of the unknown-position component. In a different manner, researchers in [16] propose an original method that uses communication to a moving target to refine the solution area. Alternatively, dynamic approaches based on the sequential Monte-Carlo technique [17] have been proposed in [18], [19], and [20]. A mobility model is added to the observation of anchors in order to improve the positions estimation. In these methods, every node generates a fixed number of positions called particles in order to cover the solution area. Nevertheless, these particle-filter-based methods are high memory consuming since a large amount of particles is required to achieve good performance.

In our previous work [21–23], we proposed dynamic methods using interval analysis [24–27]. These algorithms handle interval data in order to compute sensor locations. Using constraint satisfaction techniques [27–29], these methods aim to find the smallest box that covers the set of solutions. In [21] and [22], the localization problem is defined by a mobility model added to connectivity measurements considering anchors; whereas observations in [23] are set by rings equations based on received signal strength indicator (RSSI) comparisons [30–32]. In this paper we propose an original decentralized dynamic method based on intervals. The novelty of this method remains in the way that it defines observations considering all the sensors in the network. In other words, it employs measurements to both anchors and nonanchor nodes. The observation constraints are defined as rings equations using RSSI comparisons. The major advantage of this method is that it works reliably in low-anchor density networks. While anchor-based approaches restrict environment conditions such as uniformly deployed anchors, the proposed method relaxes these assumptions in a guaranteed way. Extensive simulations are then run showing better performance of our method than anchor-based methods especially in networks where only few sensors are equipped with GPS.

The rest of this paper is organized as follows. In Section II we define the localization problem setting mobility and observation constraints. In Section III we briefly present the theory of interval analysis. We then expose the interval-based solution of the problem. The performances of our method are illustrated with simulation results in Section IV. Finally, Section V concludes the paper.

II. PROBLEM STATEMENT

The proposed method defines two types of sensors deployed in the network, anchors and nonanchor nodes (or simply nodes). Anchors are equipped with positioning hardware such as GPS. They are aware of their positions, whereas nonanchor nodes do not know their locations and thus need to be implemented with the localization algorithm. The proposed method takes advantage of the mobility of the node to set the problem constraints. It thus involves a mobility model to refine the localization problem. Besides the mobility model, it uses measurements to both anchors and nonanchor nodes. In the following, we define the mobility and the observation models describing the localization problem.

A. Mobility Model

Sensors are deployed in a dynamic field of interest where they are moving in an uncontrollable manner. Many mobility models have been proposed in literature to describe their motion [33–35]. In our method we aim to use a basic mobility model in the way that the algorithm remains general and thus applicable to as many situations as possible. A simple mobility model with minimum assumptions is the random walk mobility model. It assumes that only the maximal velocity $v_{\max}$ of nodes is known. Between two time steps, the node is able to move in any direction with a velocity less than $v_{\max}$, which means that the distance traveled by the node over 1 s is less than $v_{\max}$. Hence, the mobility equation is formulated as follows,

$$(x_1(t) - x_1(t-1))^2 + (x_2(t) - x_2(t-1))^2 \leq v_{\max}^2 \quad (1)$$

where $x_1(t)$ and $x_2(t)$ are the coordinates of the considered mobile node at time t. The time period is supposed equal to 1 s. Any additional details on nodes mobility could be added to refine the model. Knowing the punctual position of the considered node at time $t-1$, the mobility constraint given by (1) is a disk equation whose radius is $v_{\max}$.

B. Observation Model using RSSI Comparison

1) *Introduction*: The motivation of the method is to compute accurate locations in a network where only a few sensors are equipped with GPS. For this purpose, the proposed observation model involves all sensors within the vicinity of the considered node, including other nodes. That is, at each time step, the considered node collects measurements from the anchors and the nonanchor nodes located within its communication range. The observations are rings equations centered on the detected sensors. Their inner and outer radii are defined using comparison of RSSI [23, 30, 31]. Using RSSI comparison, the method avoids the estimation of the channel pathloss model, which links the distance traveled by a signal to its strength.

Each ring centered on a specific sensor is generated by a comparison of the strengths of the signals sent by the sensor and received by all others. This approach assumes that the strength of a signal decreases monotonically as the traveled distance by the signal increases. Practically, each sensor broadcasts signals with the same initial strength P_0 in the network. Other sensors receive these messages with different RSSI, depending on their distances

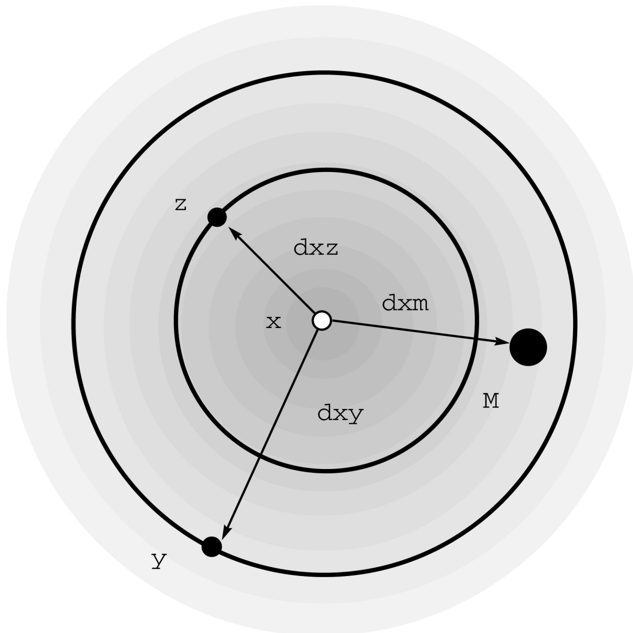

Fig. 1. Rings generation using RSSI comparison.

to the sender. Assume that M is the considered mobile node, X is the sensor sending signals, and Y and Z are two other sensors of the network. Let $\mathrm{RSSI}_{X,Y}$, $\mathrm{RSSI}_{X,M}$ and $\mathrm{RSSI}_{X,Z}$ be the strengths of the signals sent by X and received by Y, M, and Z respectively. Hence, if $\mathrm{RSSI}_{X,Y} < \mathrm{RSSI}_{X,M} < \mathrm{RSSI}_{X,Z}$, then $d(X,Y) > d(X,M) > d(X,Z)$ where $d(\cdot,\cdot)$ is the Euclidean distance operator. The node M is thus likely to fall within the ring centered on X and of radii $d(X,Z)$ and $d(X,Y)$ as shown in Fig. 1. Therefore, the generation of rings is tightly related to the positions of the involved sensors.

2) *Observation Equations*: The definition of rings requires the knowledge of sensors positions. This might be a drawback for rings involving nonanchor nodes since their positions are unknown. Moreover, the incertitude over nodes positions yields an incertitude over rings and thus larger rings than they should be in reality. In order to avoid losing relevant information, the key idea of the method is to generate series of rings definitions, each using either anchors or nodes. Consider that I and J are the set of indices of all anchors and nodes within the vicinity of M, respectively. Each sensor $\mathbf{s}_k$, $k \in \{I \cup J\}$, broadcasts signals in the network with a fixed initial strength. According to the RSSI measurements over anchors, a first definition of the ring radii is established. Indices of selected anchors to define the inner and outer radii, $l_{A,k}$ and $h_{A,k}$ respectively, are as follows,

$$\begin{aligned} l_{A,k} &= \arg\{\min_{i\in I_k}\{\mathrm{RSSI}_{\mathbf{s}_k,\mathbf{a}_i} \mid \mathrm{RSSI}_{\mathbf{s}_k,\mathbf{a}_i} \geq \mathrm{RSSI}_{\mathbf{s}_k,M}\}\} \\ h_{A,k} &= \arg\{\max_{i\in I_k}\{\mathrm{RSSI}_{\mathbf{s}_k,\mathbf{a}_i} \mid \mathrm{RSSI}_{\mathbf{s}_k,\mathbf{a}_i} \leq \mathrm{RSSI}_{\mathbf{s}_k,M}\}\} \end{aligned} \tag{2}$$

where $\mathbf{a}_i$ is the ith anchor of the network and I_k is the set of indices of anchors detected by the sensor $\mathbf{s}_k$. The corresponding inner and outer radii, denoted $r_{A,k}$ and $R_{A,k}$ respectively, are given by

$$r_{A,k} = d(\mathbf{s}_k, \mathbf{a}_{l_{A,k}}), \qquad R_{A,k} = d(\mathbf{s}_k, \mathbf{a}_{h_{A,k}}). \tag{3}$$

Similarly, the strength of the considered node M is compared with the RSSI measured at nodes. A second definition of the ring is performed. The indices of the chosen nodes are defined by

$$\begin{aligned} l_{N,k} &= \arg\{\min_{j\in J_k}\{\mathrm{RSSI}_{\mathbf{s}_k,\mathbf{x}_j} \mid \mathrm{RSSI}_{\mathbf{s}_k,\mathbf{x}_j} \geq \mathrm{RSSI}_{\mathbf{s}_k,M}\}\} \\ h_{N,k} &= \arg\{\max_{j\in J_k}\{\mathrm{RSSI}_{\mathbf{s}_k,\mathbf{x}_j} \mid \mathrm{RSSI}_{\mathbf{s}_k,\mathbf{x}_j} \leq \mathrm{RSSI}_{\mathbf{s}_k,M}\}\} \end{aligned} \tag{4}$$

where $\mathbf{x}_j$ is the jth node of the network and J_k is the set of indices of nodes detected by the sensor $\mathbf{s}_k$. Note that the involved nodes should also be in the vicinity of the node M in order to exchange positions information with it. Similarly to the anchor-based ring definition, the inner and outer radii using nodes for receivers are defined as follows,

$$r_{N,k} = d(\mathbf{s}_k, \mathbf{x}_{l_{N,k}}), \qquad R_{N,k} = d(\mathbf{s}_k, \mathbf{x}_{h_{N,k}}). \tag{5}$$

Finally, the optimal inner and outer radii of each ring are deduced from elementary radii within the localization as follows,

$$r_k = \max\{r_{A,k}, r_{N,k}\}, \qquad R_k = \min\{R_{A,k}, R_{N,k}\}. \tag{6}$$

Note that observation messages do not include radii values, but the indices l_A, l_N, h_A, and h_N corresponding to either anchors or nodes. Coordinates of involved anchors are also exchanged within observation messages. During the localization process, the considered node communicates with the specified nonanchor nodes to get their positions and set the rings equations as follows,

$$r_k^2 \leq (x_1(t) - s_{k,1}(t))^2 + (x_2(t) - s_{k,2}(t))^2 \leq R_k^2, \qquad k \in \{I \cup J\} \tag{7}$$

where $x_1(t)$ and $x_2(t)$ are the coordinates of the considered node and $s_{k,1}(t)$ and $s_{k,2}(t)$ are those of $\mathbf{s}_k$ at time t. Fig. 2 shows two definitions, in straight and dashed lines, of the ring centered on the anchor $\mathbf{a}_k$. Each definition is using either nodes or anchors as receivers. The final optimal ring, if nodes positions are considered to be punctual, is given in bold line.

III. INTERVAL-BASED ALGORITHM

The self-localization of sensors is a key problem of mobile sensor networks. In this paper we resolve the problem using interval analysis [24, 27]. In the following, we first recall the basic concepts of interval analysis. We then expose the resolution of the problem using intervals.

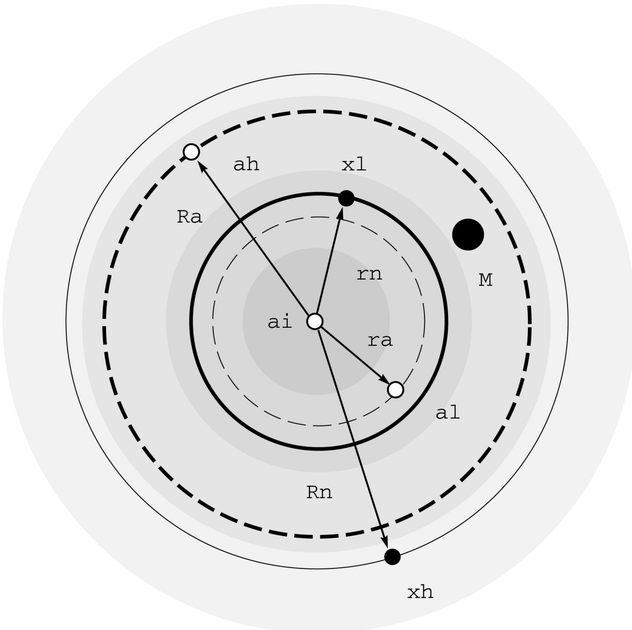

Fig. 2. Rings definition using anchors and nonanchor nodes.

A. Interval Analysis

The field of interval analysis is a relatively recent branch of mathematics [24, 27]. It has important applications such as solving global optimization problems in a guaranteed way. The guaranteed aspect remains in the way that the interval result will contain the entire set of punctual solutions. Interval analysis is based upon the very simple idea of enclosing real numbers in intervals and vectors in multi-dimensional boxes. A real interval, $[x] = [\underline{x}, \bar{x}]$, is a closed subset of $\mathbb{R}$, defined as follows,

$$[x] = [\underline{x}, \bar{x}] = \{x \in \mathbb{R} \mid \underline{x} \leq x \leq \bar{x}\} \tag{8}$$

where $\underline{x}$ and $\bar{x}$ are the lower and upper endpoints of the interval. An interval can be identified by its center $c([x]) = (\underline{x} + \bar{x})/2$ and its width $w([x]) = \bar{x} - \underline{x}$, as well. A multi-dimensional interval, also called box, is defined by the Cartesian product of real intervals as follows,

$$\begin{aligned}[\mathbf{x}] &= [x_1] \times \cdots \times [x_n] = [\underline{x}_1, \bar{x}_1] \times \cdots \times [\underline{x}_n, \bar{x}_n] \\ &= \{(x_1, \ldots, x_n) \in \mathbb{R}^n \mid \underline{x}_i \leq x_i \leq \bar{x}_i, 1 \leq i \leq n\}.\end{aligned} \tag{9}$$

An interval has a dual nature as both a number and a set of real numbers [24, 27, 25]. The interval theory makes use of this duality to extend arithmetic and set operations for intervals. For instance, if we consider the set difference operator, an interval $[x]$ deprived of an interval $[y]$ is an interval given by

$$[x] \setminus [y] = [\{x \in [x] \mid x \notin [y]\}]. \tag{10}$$

All set operations defined for intervals could be extended to boxes. Then, a box $[\mathbf{x}]$ deprived of a box $[\mathbf{y}]$ yields a box, $[\mathbf{z}] = [\mathbf{x}] \setminus [\mathbf{y}]$, whose coordinates $i \in \{1, \ldots, n\}$ are given by

$$[z_i] = \begin{cases} [x_i] \setminus [y_i] & \text{if} \quad [x_k] \subseteq [y_k], \quad 1 \leq k \leq n, \quad k \neq i \\ [x_i] & \text{otherwise} \end{cases}. \tag{11}$$

In the same manner, the main classical arithmetic operations, namely addition (+), substraction (−), multiplication (∗), and division (/), are extended to real intervals and boxes.

Similarly to operators, all functions could be applied to intervals. Consider a function $\mathbf{f} : \mathbf{x} \in \mathbb{R}^n \longmapsto \mathbf{f}(\mathbf{x}) \in \mathbb{R}^m$. Applying $\mathbf{f}$ to a box $[\mathbf{x}] \subseteq \mathbb{R}^n$ is a set given by $\mathbf{f}([\mathbf{x}]) = \{\mathbf{f}(\mathbf{x}) \mid \mathbf{x} \in [\mathbf{x}]\}$. The resulting set is not necessarily a connected interval, which leads to the inclusion functions. An inclusion function of $\mathbf{f}$, denoted $[\mathbf{f}]$, computes a box of $\mathbb{R}^m$ enclosing $\mathbf{f}([\mathbf{x}])$, $\mathbf{f}([\mathbf{x}]) \subseteq [\mathbf{f}]([\mathbf{x}])$. This is the so-called wrapping effect. It is obvious that a function has an infinite number of inclusion functions. The minimal inclusion function, denoted $[\mathbf{f}]^*$, leads to the smallest box containing $\mathbf{f}([x])$.

Using intervals theory, it becomes possible to achieve tasks often thought to be out of the reach of numerical methods. Let $\mathbf{x}$ be a variable of $\mathbb{R}^n$ and $\mathbf{f}$ a function defined from $\mathbb{R}^n$ to R^m, then $\mathbf{f}(\mathbf{x}) = \mathbf{0}$ is a set of constraints. If $\mathbf{x} \in [\mathbf{x}]$, then $\mathcal{H} : (\mathbf{f}(\mathbf{x}) = 0, \mathbf{x} \in [\mathbf{x}])$ is called a constraint satisfaction problem (CSP) [27]. In the interval framework, resolving this problem leads to a box included in $[\mathbf{x}]$. The solution box is obtained by contracting the initial domain $[\mathbf{x}]$ using a specific algorithm, called contractor [27, 26]. In this paper, we use the Waltz contractor [28]. Being a forward-backward algorithm, it iterates all constraints without any prior order, until no contraction is possible. Although it leads to local minimal boxes, the Waltz contractor remains a simple low-cost algorithm that works efficiently on the localization problem presented in this paper.

B. Proposed Algorithm using Intervals

Consider that $x_1(t)$ and $x_2(t)$ are the coordinates of the considered node at time t and I and J are the indices set of all anchors and nodes within its communication range, respectively. The localization problem at time t is then defined by both the mobility and the observation models given by

$$(x_1(t) - x_1(t-1))^2 + (x_2(t) - x_2(t-1))^2 \leq v_{\max}^2 \tag{12}$$

$$\begin{aligned} r_i^2 \leq (x_1(t) - a_{i,1}(t))^2 + (x_2(t) - a_{i,2}(t))^2 \leq R_i^2, \qquad i \in I \\ r_j^2 \leq (x_1(t) - x_{j,1}(t))^2 + (x_2(t) - x_{j,2}(t))^2 \leq R_j^2, \qquad j \in J \end{aligned} \tag{13}$$

where $v_{\max}$ is the maximal velocity of the considered node, $a_{i,1}(t)$ and $a_{i,2}(t)$ are the coordinates of the ith anchor at time t, $x_{j,1}(t)$, and $x_{j,2}(t)$ are the coordinates of the jth node and r_i, R_i, r_j and R_j are the final radii

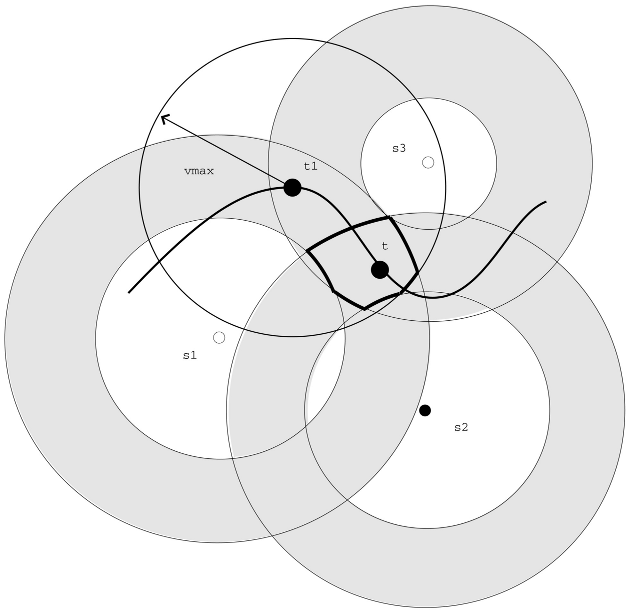

Fig. 3. Solution area of localization problem using rings definition.

of observation rings as shown in Section IIB. An illustration of such a problem is given in Fig. 3 where the position of the node $\mathbf{x}_2$ is considered to be known and punctual.

In general, the localization problem does not have a single solution, but an infinite set of solutions covering a bounded area. While most existing approaches aim to choose one punctual position within the solution area, interval-based methods compute an optimal outer domain bounding all possible solutions. Estimated positions are boxes where the exact positions certainly exist. With interval methods, the propagation of the computed positions leads to a bounded cumulative error during the estimation process.

The key idea of our technique is to define nodes locations as two-dimensional intervals $[\mathbf{x}]$. Resolving the localization problem in the interval framework consists of defining it as a CSP and then finding solutions using the Waltz contractor. For this purpose, at each time step, an initial box is defined using the mobility equation formulated with intervals as follows,

$$[[x_1](t) - [x_1](t-1)]^2 + [[x_2](t) - [x_2](t-1)]^2 = [0, v_{\max}^2]. \tag{14}$$

This leads to two primitive functions given by

$$\begin{aligned} [x_1](t) &= [[x_1](t-1) - [b_1](t)] \sqcup [[x_1](t-1) + [b_1](t)] \\ [x_2](t) &= [[x_2](t-1) - [b_2](t)] \sqcup [[x_2](t-1) + [b_2](t)] \end{aligned} \tag{15}$$

where

$$[b_1](t) = \left[\sqrt{v_{\max}^2 - [[x_2](t) - [x_2](t-1)]^2}\right]$$

$$[b_2](t) = \left[\sqrt{v_{\max}^2 - [[x_1](t) - [x_1](t-1)]^2}\right].$$

The previous position box, $[\mathbf{x}](t-1)$, is propagated with the disk equation above. Extending a box using a disk equation yields a rounded corner box as shown in Fig. 4(a) in dashed line. Expressing the result using intervals leads to the minimal box $[\mathbf{x}]^*(t)$ enclosing it. It could also be obtained using a square equation whose sides are equal to $v_{\max}$ as shown in Fig. 4(b). Consequently, we are able to simplify the propagation primitive equations to square equations as follows,

$$\begin{aligned} [x_1](t) &= [x_1](t-1) + [-v_{\max}, v_{\max}] \\ [x_2](t) &= [x_2](t-1) + [-v_{\max}, v_{\max}]. \end{aligned} \tag{16}$$

The initial domain is then contracted by the Waltz algorithm using observation and mobility constraints without any prior order. During the localization process, the considered mobile node collects measurements from sensors within its vicinity and then communicates with the nodes specified in the observation messages in order to get their positions at each iteration of the process. For every

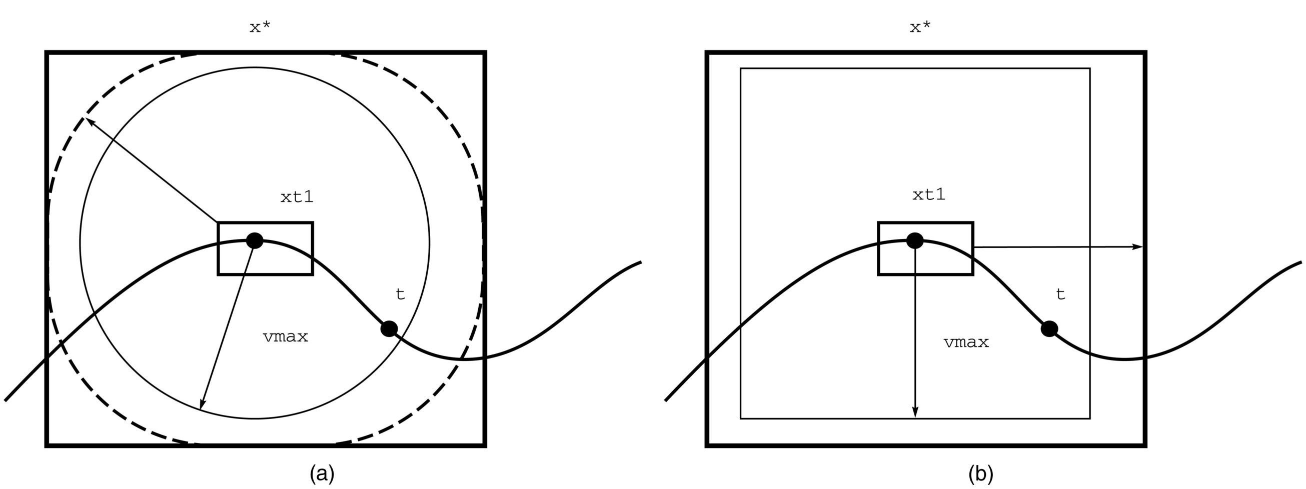

Fig. 4. Propagation of previous box $[\mathbf{x}](t-1)$ using mobility disk equation in (a) and approximated square equation in (b).

detected anchor $\mathbf{a}_i$, $i \in I$, the inner and outer radii of the corresponding ring are given by

$$\begin{aligned}
r_{A,i} &= \sqrt{(a_{i,1}(t) - a_{l_{A,i},1}(t))^2 + (a_{i,2}(t) - a_{l_{A,i},2}(t))^2} \\
R_{A,i} &= \sqrt{(a_{i,1}(t) - a_{h_{A,i},1}(t))^2 + (a_{i,2}(t) - a_{h_{A,i},2}(t))^2} \\
r_{N,i} &= \min\left[\sqrt{[a_{i,1}(t) - [x_{l_{N,i},1}](t)]^2 + [a_{i,2}(t) - [x_{l_{N,i},2}](t)]^2}\right] \\
R_{N,i} &= \max\left[\sqrt{[a_{i,1}(t) - [x_{h_{N,i},1}](t)]^2 + [a_{i,2}(t) - [x_{h_{N,i},2}](t)]^2}\right] \\
r_i &= \max\{r_{A,i}, r_{N,i}\}, \qquad R_i = \min\{R_{A,i}, R_{N,i}\}
\end{aligned} \tag{17}$$

$l_{A,i}$, $l_{N,i}$, $h_{A,i}$, and $h_{N,i}$ being the indices of anchors and nodes given in the observation message sent by the anchor i. Note that the minimal bound of an interval-inner radius is chosen to avoid losing the guaranteed aspect of the method. For the same reason, maximal bounds of interval-outer radii are used as well. The observations equations based on anchors are then given by

$$[[x_1](t) - a_{i,1}(t)]^2 + [[x_2](t) - a_{i,2}(t)]^2 = [r_i^2, R_i^2], \qquad i \in I. \tag{18}$$

Similarly, for each detected node $\mathbf{x}_j, j \in J$, the corresponding inner and outer radii are given by

$$\begin{aligned}
r_{A,j} &= \min\left[\sqrt{[[x_{j,1}](t) - a_{l_{A,j},1}(t)]^2 + [[x_{j,2}](t) - a_{l_{A,j},2}(t)]^2}\right] \\
R_{A,j} &= \max\left[\sqrt{[[x_{j,1}](t) - a_{h_{A,j},1}(t)]^2 + [[x_{j,2}](t) - a_{h_{A,j},2}(t)]^2}\right] \\
r_{N,j} &= \min\left[\sqrt{[[x_{j,1}](t) - [x_{l_{N,j},1}](t)]^2 + [[x_{j,2}](t) - [x_{l_{N,j},2}](t)]^2}\right]
\end{aligned} \tag{19}$$

$$\begin{aligned}
R_{N,j} &= \max\left[\sqrt{[[x_{j,1}](t) - [x_{h_{N,j},1}](t)]^2 + [[x_{j,2}](t) - [x_{h_{N,j},2}](t)]^2}\right] \\
r_j &= \max\{r_{A,j}, r_{N,j}\}, \qquad R_j = \min\{R_{A,j}, R_{N,j}\}.
\end{aligned}$$

$l_{A,j}$, $l_{N,j}$, $h_{A,j}$, and $h_{N,j}$ are the indices of anchors and nodes given in the observation message sent by the node j. The corresponding observations equations are given by

$$[[x_1](t) - [x_{j,1}](t)]^2 + [[x_2](t) - [x_{j,2}](t)]^2 = [r_j^2, R_j^2], \qquad j \in J. \tag{20}$$

In order to implement (18) and (20) in the Waltz algorithm, primitive constraints should be generated. Each observation yields couples of primitive equations, based on either the outer or the inner radii limitations. Starting with anchors observations, the primitive constraints derived from outer radii are given by

$$\begin{aligned}
[x_1](t) &= [a_{i,1}(t) - [b_{i,1}](t)] \sqcup [a_{i,1}(t) + [b_{i,1}](t)] \\
[x_2](t) &= [a_{i,2}(t) - [b_{i,2}](t)] \sqcup [a_{i,2}(t) + [b_{i,2}](t)]
\end{aligned} \tag{21}$$

where

$$\begin{aligned}
[b_{i,1}](t) &= \left[\sqrt{R_i^2 - [[x_2](t) - a_{i,2}(t)]^2}\right] \\
[b_{i,2}](t) &= \left[\sqrt{R_i^2 - [[x_1](t) - a_{i,1}(t)]^2}\right].
\end{aligned}$$

In order to take advantage of the inner radii constraints, we must deprive the position box $[\mathbf{x}]$ of the circles of radii r_i, $i \in I$. Using intervals, the problem consists of depriving $[\mathbf{x}]$ of the square boxes $[\mathbf{z}_i]$ inscribed in these circles. The boxes coordinates are given by

$$\begin{aligned}
[z_{i,1}] &= \left[a_{i,1}(t) - r_i\frac{\sqrt{2}}{2}, a_{i,1}(t) + r_i\frac{\sqrt{2}}{2}\right] \\
[z_{i,2}] &= \left[a_{i,2}(t) - r_i\frac{\sqrt{2}}{2}, a_{i,2}(t) + r_i\frac{\sqrt{2}}{2}\right].
\end{aligned}$$

The corresponding constraints are eventually formulated by

$$[\mathbf{x}] = [\mathbf{x}] \setminus [\mathbf{z}_i], \qquad i \in I. \tag{22}$$

In the same manner, when using nodes observations, outer radii primitive constraints are given by

$$\begin{aligned}
[x_1](t) &= [[x_{j,1}](t) - [b_{j,1}](t)] \sqcup [[x_{j,1}](t) + [b_{j,1}](t)] \\
[x_2](t) &= [[x_{j,2}](t) - [b_{j,2}](t)] \sqcup [[x_{j,2}](t) + [b_{j,2}](t)]
\end{aligned} \tag{23}$$

where $j \in J$ and

$$\begin{aligned}
[b_{j,1}](t) &= \left[\sqrt{R_j^2 - [[x_2](t) - [x_{j,2}](t)]^2}\right] \\
[b_{j,2}](t) &= \left[\sqrt{R_j^2 - [[x_1](t) - [x_{j,1}](t)]^2}\right].
\end{aligned}$$

The position boxes should also be deprived from the smallest squares inscribed in the inner circles of different nodes rings. These square boxes have as coordinates

$$[z_{j,1}] = \left[\max\left[[x_{j,1}](t) - r_j\frac{\sqrt{2}}{2}\right], \min\left[[x_{j,1}](t) + r_j\frac{\sqrt{2}}{2}\right]\right] \tag{24}$$

$$[z_{j,2}] = \left[\max\left[[x_{j,2}](t) - r_j\frac{\sqrt{2}}{2}\right], \min\left[[x_{j,2}](t) + r_j\frac{\sqrt{2}}{2}\right]\right].$$

This leads us to the following equation,

$$[\mathbf{x}] = [\mathbf{x}] \setminus [\mathbf{z}_j], \qquad j \in J. \tag{25}$$

Besides observations, primitive constraints derived from the mobility model (14) are also implemented in the Waltz algorithm. The pseudocode of the method is summarized in Algorithm 1. During each localization period, each node localizes itself exchanging information with other nodes at different iterations of the Waltz algorithm. The Waltz contractor iterates all constraints until the position box of the considered node is no longer changing. An illustration

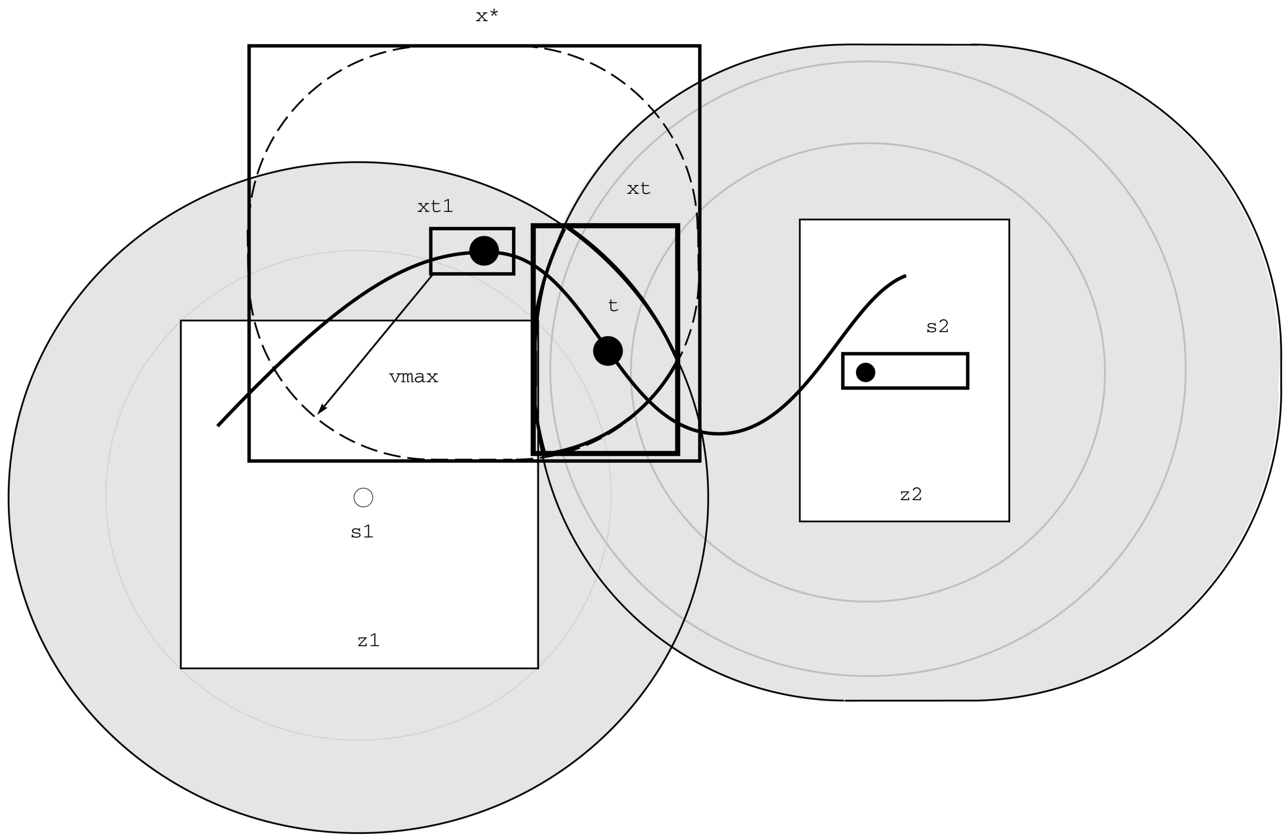

Fig. 5. An illustration of localization result with interval-based method.

of the resulting position box is given in Fig. 5. The obtained box is much smaller than the one involving only the anchor-based constraint. Note that extending the box of the node $\mathbf{x}_j$ by its outer disk equation does not yield a disk, but a larger rounded corner box. Since inner disks constraints also yield boxes, the so-called rings are thus distorted rings as shown in Fig. 5.

ALGORITHM 1 *Proposed method using anchors and nodes*

Input: Initial domain $[x_1]_0$ and $[x_2]_0$, $v_{\max}$, observation messages
Output: $[x_1]$ and $[x_2]$
Initialization: $[x_1](0) \leftarrow [x_1]_0, [x_2](0) \leftarrow [x_2]_0$;
for $t \leq T$ **do**
  $[x_1](t) = [x_1](t-1) + [-v_{\max}, v_{\max}]$;
  $[x_2](t) = [x_2](t-1) + [-v_{\max}, v_{\max}]$;
  while contraction is positive **do**
    for $i \in I$ **do**
      $R_{A,i} = \sqrt{(a_{i,1}(t) - a_{h_{A,i},1}(t))^2 + (a_{i,2}(t) - a_{h_{A,i},2}(t))^2}$;
      $R_{N,i} = \max\left[\sqrt{[a_{i,1}(t) - [x_{h_{N,i},1}](t)]^2 + [a_{i,2}(t) - [x_{h_{N,i},2}](t)]^2}\right]$;
      $R_i = \min\{R_{A,i}, R_{N,i}\}$;
      $[b_{i,1}](t) = \left[\sqrt{R_i^2 - [[x_2](t) - a_{i,2}(t)]^2}\right]$; $[x_1](t) = [x_1](t) \cap [[a_{i,1}(t) - [b_{i,1}](t)] \sqcup [a_{i,1}(t) + [b_{i,1}](t)]]$;
      $[b_{i,2}](t) = \left[\sqrt{R_i^2 - [[x_1](t) - a_{i,1}(t)]^2}\right]$; $[x_2](t) = [x_2](t) \cap [[a_{i,2}(t) - [b_{i,2}](t)] \sqcup [a_{i,2}(t) + [b_{i,2}](t)]]$;
      $r_{A,i} = \sqrt{(a_{i,1}(t) - a_{l_{A,i},1}(t))^2 + (a_{i,2}(t) - a_{l_{A,i},2}(t))^2}$;
      $r_{N,i} = \min\left[\sqrt{[a_{i,1}(t) - [x_{l_{N,i},1}](t)]^2 + [a_{i,2}(t) - [x_{l_{N,i},2}](t)]^2}\right]$;
      $r_i = \max\{r_{A,i}, r_{N,i}\}$;

$$[z_{i,1}] = \left[a_{i,1}(t) - r_i\frac{\sqrt{2}}{2}, a_{i,1}(t) + r_i\frac{\sqrt{2}}{2}\right];\ [z_{i,2}] = \left[a_{i,2}(t) - r_i\frac{\sqrt{2}}{2}, a_{i,2}(t) + r_i\frac{\sqrt{2}}{2}\right];$$

$[\mathbf{z}_i] = [z_{i,1}] \times [z_{i,2}];\ [\mathbf{x}](t) = [x_1](t) \times [x_2](t);\ [\mathbf{x}](t) = [\mathbf{x}](t) \setminus [\mathbf{z}_i];$

end

for $j \in J$ **do**

$$R_{A,j} = \max\left[\sqrt{[[x_{j,1}](t) - a_{h_{A,j},1}(t)]^2 + [[x_{j,2}](t) - a_{h_{A,j},2}(t)]^2}\right];$$

$$R_{N,j} = \max\left[\sqrt{[[x_{j,1}](t) - [x_{h_{N,j},1}](t)]^2 + [[x_{j,2}](t) - [x_{h_{N,j},2}](t)]^2}\right];$$

$R_j = \min\{R_{A,j}, R_{N,j}\};$

$$[b_{j,1}](t) = \left[\sqrt{R_j^2 - [[x_2](t) - [x_{j,2}](t)]^2}\right];\ [x_1](t) = [x_1](t) \cap [[[x_{j,1}](t) - [b_{j,1}](t)] \sqcup [[x_{j,1}](t) + [b_{j,1}](t)]];$$

$$[b_{j,2}](t) = \left[\sqrt{R_j^2 - [[x_1](t) - [x_{j,1}](t)]^2}\right];\ [x_2](t) = [x_2](t) \cap [[[x_{j,2}](t) - [b_{j,2}](t)] \sqcup [[x_{j,2}](t) + [b_{j,2}](t)]];$$

$$r_{A,j} = \min\left[\sqrt{[[x_{j,1}](t) - a_{l_{A,j},1}(t)]^2 + [[x_{j,2}](t) - a_{l_{A,j},2}(t)]^2}\right];$$

$$r_{N,j} = \min\left[\sqrt{[[x_{j,1}](t) - [x_{l_{N,j},1}](t)]^2 + [[x_{j,2}](t) - [x_{l_{N,j},2}](t)]^2}\right];$$

$r_j = \max\{r_{A,j}, r_{N,j}\};$

$$[z_{j,1}] = \left[\max\left[[x_{j,1}](t) - r_j\frac{\sqrt{2}}{2}\right], \min\left[[x_{j,1}](t) + r_j\frac{\sqrt{2}}{2}\right]\right];\ [z_{j,2}] = \left[\max\left[[x_{j,2}](t) - r_j\frac{\sqrt{2}}{2}\right], \min\left[[x_{j,2}](t) + r_j\frac{\sqrt{2}}{2}\right]\right];$$

$[\mathbf{z}_j] = [z_{j,1}] \times [z_{j,2}];\ [\mathbf{x}](t) = [x_1](t) \times [x_2](t);\ [\mathbf{x}](t) = [\mathbf{x}](t) \setminus [\mathbf{z}_j];$

end

$$[b_1](t) = \left[\sqrt{v_{\max}^2 - [[x_2](t) - [x_2](t-1)]^2}\right];\ [x_1](t) = [x_1](t) \cap [[[x_1](t-1) - [b_1](t)] \sqcup [[x_1](t-1) + [b_1](t)]];$$

$$[b_2](t) = \left[\sqrt{v_{\max}^2 - [[x_1](t) - [x_1](t-1)]^2}\right];\ [x_2](t) = [x_2](t) \cap [[[x_2](t-1) - [b_1](t)] \sqcup [[x_2](t-1) + [b_2](t)]];$$

end

end

IV. SIMULATIONS

In order to evaluate the effectiveness of the proposed method, we generate a sine-based trajectory and we move all sensors using a reference point group mobility (RPGM) model [33–35]. According to this model, each mobile sensor is given a predefined reference trajectory (e.g. a sinusoidal motion path). Mobile sensors are then allowed to move randomly around their reference trajectories. An illustration of such a model is given in Fig. 6. This plot shows 10 anchors and 30 nodes deployed initially in a 100 m $\times$ 100 m area and then moving according to the RPGM model for a total period of 100 s. The maximal velocity of the nodes is equal to 3.169 m/s according to the chosen model. In Algorithm 1, we first compare our method with a Monte-Carlo based method. We then compare it with an interval-based method using only anchors information.

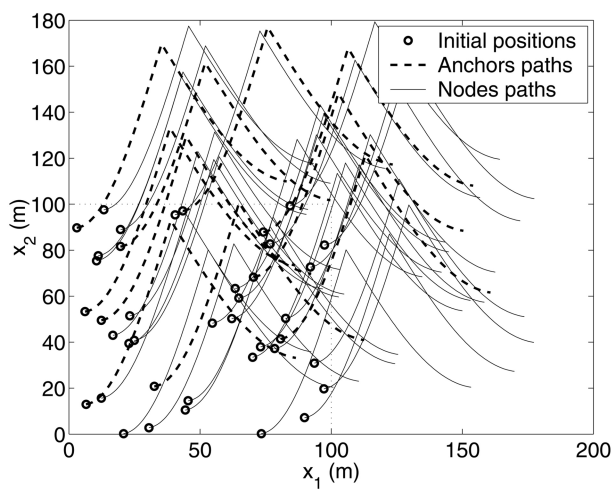

Fig. 6. Illustration of reference group mobility model.

A. Comparison with a Monte-Carlo-Based Method

In this section we compare our method with the Monte-Carlo boxed (MCB) localization method proposed in [19]. It is an anchor-based method using a sequential Monte-Carlo (particle filter) approach [17]. The rationale behind this approach consists of generating a fixed number of particles covering the solution area. At every time step, each mobile node collects connectivity information from anchors within its vicinity and then sets a closed area where it generates randomly N_p positions, called particles. The estimated position is thus defined as the barycenter of the generated particles. All particles are then kept in the memory in order to be used in the following localization step. In order to compare our method with the MCB method, we move 3 anchors and 5 nodes within the 100 m $\times$ 100 m area using the RPGM model given in Fig. 6. The anchors and nodes are chosen to be within the communication range of each

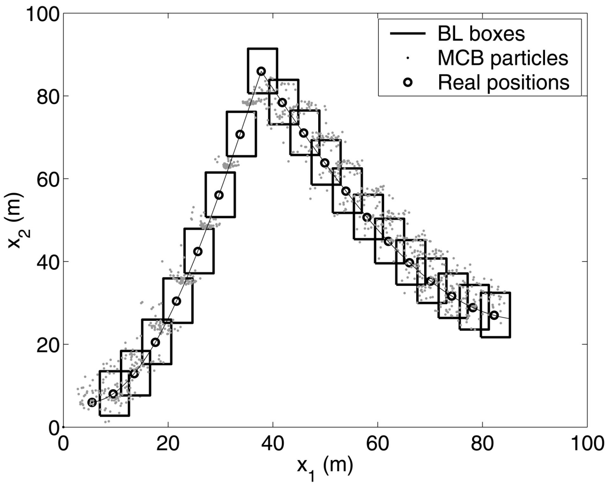

Fig. 7. Comparison of our method (BL) with the Monte-Carlo-based method (MCB).

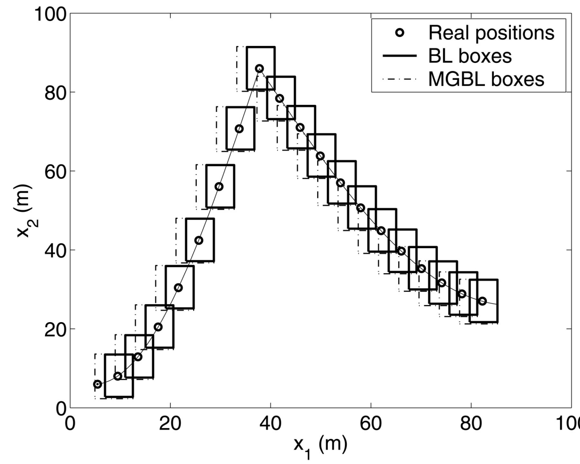

Fig. 9. Comparison of our proposed method (BL) to the anchor-based method (MGBL).

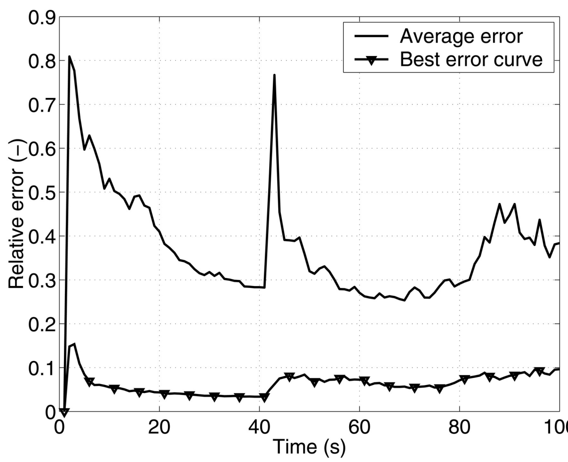

Fig. 8. Best and average ratio curves of errors obtained with our method over those obtained with the MCB method.

others in all time steps. The communication range is set to 10 m, which is used in the definition of the proximity measurements. On the other hand, the maximal velocity of the sensors is set to its real value 3.169 m/s and the number of particles of the MCB method is set to 50 particles.

Fig. 7 shows the position boxes and the particles obtained using both methods for tracking one mobile node. The average computation time per node over the 100 time steps is equal to 1.1076 s with the proposed method and to 1.2542 s with the MCB technique; whereas the average errors per node and per time step are equal to 1.61 m and to 5.4532 m, respectively. Note that the position boxes obtained with our method contain the real positions at all time steps, which corroborates the guaranteed aspect of our method; whereas the MCB particles do not cover the real positions at almost all the time steps. Fig. 8 shows the average ratio curve of the errors obtained with our method over those obtained using MCB. It shows the best ratio curve of errors corresponding to the node with the least relative error, as well. Note that the localization results are highly correlated to the deployment of anchors and nodes around the tracked node. The offset between the best and the average relative error curves shows that even with the same number of nodes and anchors in their vicinity, the localization performance is different between the nodes and also varying over the time. It is worth noting that, besides the increase of the estimation accuracy, the proposed method ensures less consumption of the memory resources compared with MCB since only one position box is kept in the memory at every time step.

B. Comparison of the Proposed Method with the Model-Free Anchor-Based Method

In this section, we compare the proposed method with the rings overlapping method using only observations to anchors, proposed in [23]. For this purpose, we move 3 anchors and 5 nodes as in Section IVA. All the sensors are able to communicate with each others at every time step. Fig. 9 shows the position boxes obtained using our method (BL) and the anchor-based method (MGBL) corresponding to the localization of one mobile node. The plot shows that the boxes obtained with BL are always included in those obtained with MGBL, leading to more accuracy of the estimation process. The average computation time per node over all the time steps is equal to 1.1076 s with our method and to 0.568 s with the MGBL method. Although the computation time increases, the estimation error decreases for all the nodes. Fig. 10 shows the average ratio curves of the boxes areas and the estimation errors obtained with our method over those obtained with MGBL. It shows as well the best ratio curves of areas and errors corresponding to the node having the least relative estimation error. The difference between the average and the best curves shows that the localization

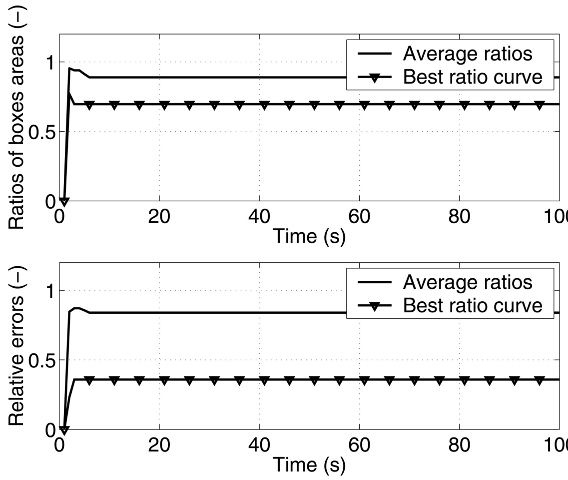

Fig. 10. Ratio curves of boxes areas and estimation errors computed with proposed method over those computed using anchor-based method.

results vary from one node to another depending on the deployment of anchors and nodes around them.

In the following, we aim at computing the increase of the energy consumption in one time step. Assume that the network is composed of m anchors and n nodes all of them communicating with each other. This increase is mainly due to the transmission of messages during the algorithm computation, to the reception and the sending of the observation messages and to the exchange of signals in the measurements generation phase.

Concerning transmission within the algorithm, each node sends its coordinates once at each iteration to all the nodes neighboring it. Moreover, in this example, the Waltz algorithm is very fast, leading to the final box in around 2 iterations per time step on average. In other words, it sends twice its coordinates to $(n-1)$ sensors. The coordinates consist of two real intervals and thus 4 real numbers. If we consider that a real number is coded using 8 bits, then the coordinates consist of $4*8 = 32$ bits. Therefore, a node sends $2*(n-1)*32 = 64*(n-1)$ bits per time step. On the other hand, each node needs the coordinates of the other nodes since it uses them in its algorithm. It thus receives coordinates of $(n-1)$ nodes twice per time step. This leads to a reception of $(n-1)*2*32 = 64*(n-1)$ bits. At last, if we consider only the transmission costs during the algorithm, a node sends $64*(n-1)$ bits and receives $64*(n-1)$ bits. Let P_s and P_r be the amount of energy consumption for sending and receiving one bit, respectively. Hence, the energy consumption of a node increases about $P_s*64*(n-1)+P_r*64*(n-1) = 64*(n-1)*(P_s+P_r)$ with respect to the anchor-based method.

If we consider now the reception of measurements, anchors messages will contain in addition the indices of nodes used to define the inner and outer radii of the nodes rings. Then it receives 2 additional integers in an anchor message, which means the reception of $m*2*8 = 16*m$ bits. A node also receives messages from other nodes. These messages contain the identifier of the sender, the coordinates of anchors used for the anchor ring, and the indices of the nodes used for the node ring. This leads to $(1+2*2+2*1)*8 = 56$ bits. Since it receives messages from $(n-1)$ nodes, then it receives $56*(n-1)$ bits. It receives thus $56*(n-1)+16*m$ bits more. It also sends measurements to all other nodes, which means that it sends $56*(n-1)$ bits. Hence, the energy consumption increases $P_s*56*(n-1)+P_r*(56*(n-1)+16*m)$ with respect to the anchor-based method for the exchange of measurements.

Consider now the measurements generation. For anchors observation messages, no additional signals are exchanged with nodes. The increase remains in the generation of nodes measurements. If we consider the case of a sender node generating the measure, it broadcasts signals in the network including its identifier (1 number). It sends at minimal $m+n-1$ signals in the network, which means sending $(m+n-1)*8$ bits. Anchors and nodes receive the signals, measure the RSSIs, and send them back to the sender. The sender receives thus messages from $(n-1)$ nodes including the RSSIs and their identifiers, which means $(n-1)*2*8 = 16*(n-1)$ bits. It also receives messages from anchors including their two coordinates, their identifiers and their RSSIs, which leads to $m*4*8 = 32*m$ bits. A sender thus sends at minimal $(m+n-1)*8$ bits and receives $32*m+16*(n-1)$ bits. As a receiver, it receives messages from nodes with the identifiers, which means $(n-1)*8$ bits. It then measures the RSSIs and then sends these values with its identifier back to the senders, leading to sending $(n-1)*2*8 = 16*(n-1)$ bits. At last, for measurements generation, the energy consumption increases at minimal of $P_s*((m+n-1)*8+16*(n-1))+P_r*(32*m+16*(n-1)+8*(n-1)) = P_s*(8*m+24*(n-1))+P_r*(32*m+24*(n-1))$.

Finally if we compute the total increase of energy consumption for a node per time step by adding all increases, we find

$$P_s*(8*m+144*(n-1))+P_r*(48*m+144*(n-1)).$$

One then faces a trade-off between increasing the estimation accuracy by using all possible information and reducing the energy consumption as much as possible by neglecting some information.

In a second manner, we illustrate another example, where anchors are supposed to be fixed. We thus consider 5 nodes moving among the group mobility and we deploy 100 anchors in the whole 100 m $\times$ 100 m area. The disposition of anchors located within the vicinity of the nodes, as well as their number, vary from one time step to the other. Fig. 11 illustrates the

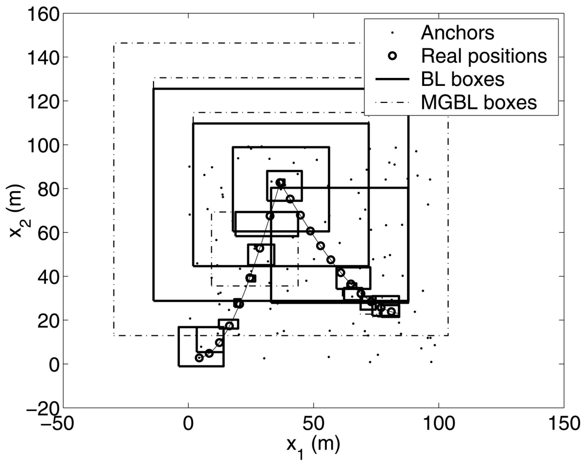

Fig. 11. Comparison of proposed method (BL) with anchor-based method (MGBL) with fixed anchors.

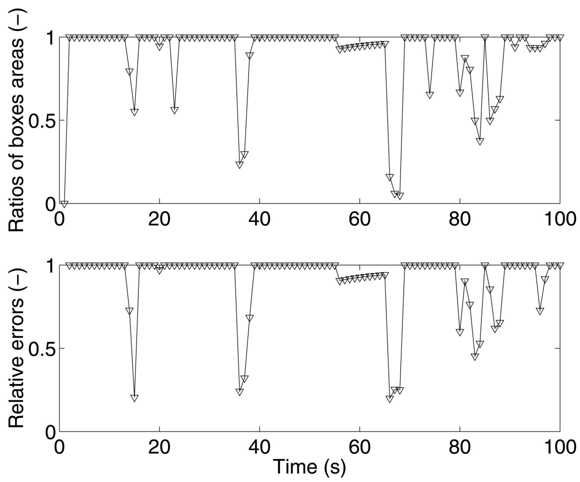

Fig. 12. Ratio curves of boxes areas and estimation errors computed with proposed method over those computed using anchor-based method with fixed anchors.

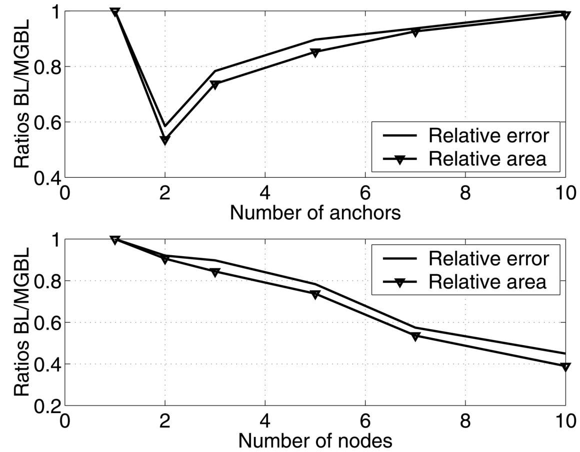

Fig. 13. Ratios of average errors and boxes areas obtained with proposed method (BL) over those obtained using anchor-based method (MGBL) varying with number of anchors and nodes deployed in the network.

boxes obtained with both BL and MGBL methods for one of the nodes chosen randomly. The plot shows that BL performs better than MGBL at many time steps, noting that it works as well as MGBL in the worst case. Fig. 12 shows the ratio curves of the boxes areas and the estimation errors obtained with BL over those obtained with MGBL for the same node. As expected, the performances of the proposed method compared with those of MGBL vary with time steps, depending on the number and the positions of the anchors around the nodes. For instance, the minimal areas ratio is obtained at instant 68, where no anchors are located within the vicinity of the considered node, whereas two of its neighbors detect 1 and 2 anchors, respectively.

C. Sensitivity to the Network Density

The effectiveness of the proposed method compared with the anchor-based method depends on the number of anchors and nodes deployed in the network. In order to illustrate this dependence, we first fix the number of nodes to 5 and we vary the number of anchors in their vicinity from 2 to 10. The top plot of Fig. 13 reports the variation of the average errors and boxes areas obtained with the proposed method over those obtained with the anchor-based method. As expected, the figure shows that the relative accuracy of the proposed method compared with the anchor-based one increases with the decrease of the anchor density in the network. This performance varies with the variation of the number of nodes, as well. Considering a fixed number of anchors equal to 3, we vary the number of nodes from 2 to 10. The bottom plot of Fig. 13 shows the ratio curves of the average error and boxes area obtained with the proposed method over those obtained with the anchor-based one. The simulation results show that the proposed method is more efficient in lower anchor density networks with more nodes compared with the anchor-based one.

V. CONCLUSION

In this paper we presented a dynamic model-free method for localization in MANETs. The guaranteed aspect of the method remains in the way that it generates interval domains covering all possible solutions of the problem. Involving both anchors and nonanchor nodes, it becomes possible to achieve the localization in low-anchor density networks. While the performances of RSSI-based methods are tightly related to the channel pathloss model, the proposed method is robust under irregular radio propagation patterns since it uses RSSI comparison. The effectiveness of the method is evaluated using simulations based on sensors moving using a group mobility model. Experimental results show that our method outperforms the anchor-based techniques in terms of accuracy. In future works, we will analyze the localization problem under inaccurate environment assumptions and sensor failure problems. The use of belief functions represents a solution to handle more consistently erroneous information communicated between the sensors.

REFERENCES

[1] Kumar, S., Zhao, F., and Shepherd, D.
Collaborative signal and information processing microsensor networks.
IEEE Signal Processing Magazine (special issue on collaborative information processing), **19**, 2 (2002).

[2] Lin, Y., Chen, B., and Varshney, P.
Decision fusion rules in multi-hop wireless sensor networks.
IEEE Transactions on Aerospace and Electronic Systems, **41**, 2 (2005), 475–488.

[3] Moges, M. and Robertazzi, R.
Wireless sensor networks: Scheduling for measurement and data reporting.
IEEE Transactions on Aerospace and Electronic Systems, **42**, 1 (2006), 327–340.

[4] Akyildiz, I. F., et al.
Wireless sensor networks: A survey.
Computer Networks, **38** (2002), 393–422.

[5] Gharavi, H. and Kumar, S. P.
Scanning the Issue: Special issue on sensor networks and applications.
Proceedings of the IEEE (special issue on sensor networks and applications), **91**, 8 (2003).

[6] Giridhar, A. and Kumar, P.R.
Computing and communication functions over sensor networks.
IEEE Journal on Selected Areas in Communications (special issue on self-organizing distributed collaborative sensor networks), **23**, 4 (2005).

[7] Luo, Z-Q., et al.
Distributed signal process in sensor networks, from the guest editors.
IEEE Signal Processing Magazine (special issue on distributed signal processing in sensor networks), **23**, 4 (2006).

[8] Hofmann-Wellenhof, B., Lichtenegger, H., and Collins, J.
Global positioning system: Theory and practice.
New York: Springer, 1994.

[9] Bulusu, N., Heidemann, J., and Estrin, D.
GPS-less low-cost outdoor localization for very small devices.
IEEE Personal Communications, **7**, 5 (2000), 28–34.

[10] Moore, D., et al.
Robust distributed network localization with noisy range measurements.
In *Proceedings of the Second ACM Conference on Embedded Networked Sensor Systems* (SenSys'04), Nov. 2004, 50–61.

[11] Lazos, L. and Poovendran, R.
Rope: Robust position estimation in wireless sensor networks.
In *Proceedings of the 4th International Symposium on Information Processing in Sensor Networks* (IPSN), 2005, 324–331.

[12] Vivekanandan, V. and Wong, V.
Concentric anchor beacon localization algorithm for wireless sensor networks.
IEEE Transactions on Vehicular Technology, **56** (2007), 2733–2744.

[13] Kaplan, L.
Global node selection for localization in a distributed sensor network.
IEEE Transactions on Aerospace and Electronic Systems, **42**, 1 (2006), 113–135.

[14] Kaplan, L.
Local node selection for localization in a distributed sensor network.
IEEE Transactions on Aerospace and Electronic Systems, **42**, 1 (2006), 136–146.

[15] Martinerie, F.
Data fusion and tracking using HMMs in a distributed sensor network.
IEEE Transactions on Aerospace and Electronic Systems, **33**, 1 (1997), 11–28.

[16] Galstyan, A., et al.
Distributed online localization in sensor networks using a moving target.
In *Proceedings of the 3rd International Symposium on Information Processing in Sensor Networks* (IPSN'04), 2004, 61–70.

[17] Doucet, A., Godsill, S., and Andrieu, C.
On sequential Monte-Carlo sampling methods for Bayesian filtering.
Statistics and Computing, **10** (2000), 197–208.

[18] Hu, L. and Evans, D.
Localization for mobile sensor networks.
Presented at the Tenth Annual International Conference on Mobile Computing and Networking (MobiCom'04), 2004.

[19] Baggio, A. and Langendoen, K.
Monte-Carlo localization for mobile wireless sensor networks.
Presented at the Second International Conference on Mobile Ad Hoc and Sensor Networks (MSN'06), 2006.

[20] Jiyoung, Y., Sungwon, Y., and Hojung, C.
Multi-hop-based Monte Carlo localization for mobile sensor networks.
Presented at the 4th Annual IEEE Communications Society Conference on Sensor, Mesh and Ad Hoc Communications and Networks (SECON'07), 2007.

[21] Mourad, F., et al.
Guaranteed boxed localization in MANETs by interval analysis and constraints propagation techniques.
Presented at IEEE GLOBECOM, 2008.

[22] Mourad, F., et al.
Anchor-based localization via interval analysis for mobile ad-hoc sensor networks.
IEEE Transactions on Signal Processing, **57**, 8 (Aug. 2009), 3226–3239.

[23] Mourad, F., et al.
Model-free interval-based localization in MANETs.
Presented at the Digital Signal Processing Workshop and 5th IEEE Signal Processing Workshop, Marco Island FL, 2009. IEEE DSP/SPE, 2009.

[24] Moore, R. E.
Methods and Applications of Interval Analysis (SIAM Studies in Applied Mathematics 2).
Philadelphia, PA: Society for Industrial and Applied Mathematics, 1987.

[25] Kearfott, R. B. and Kreinovich, V.
Applications of Interval Computations.
Norwell, MA: Kluwer Academic Publishers, 1996.

[26] Hansen, E. and Walster, G. W.
Global Optimization using Interval Analysis (2nd ed.).
New York: Marcel Dekker, 2004.

[27] Jaulin, L., et al.
Applied Interval Analysis.
New York: Springer, 2001.

[28] Waltz, D. L.
Generating semantic descriptions from drawings of scenes with shadows.
Massachusetts Institute of Technology, Cambridge, MA, Technical Report, 1972.

[29] Abdallah, F., Gning, A., and Bonnifait, P.
Box particle filtering for non linear state estimation using interval analysis.
Automatica, **44** (2008), 807–815.

[30] Liu, C., Wu, K., and He, T.
Sensor localization with ring overlapping based on comparison of received signal strength indicator.
In *Proceedings of the IEEE International Conference on Mobile Ad Hoc and Sensor Systems*, 2004, 516–518.

[31] Li, X.
RSS-based location estimation with unknown pathloss model.
IEEE Transactions on Wireless Communications, **5** (2006).

[32] Nabaee, M. and Olfat, A.
Enhanced RSS based location estimation with disk overlapping in wireless sensor networks.
Presented at the IEEE International Conference on Telecommunications (ICT'08), 2008.

[33] Camp, T., Boleng, J., and Davies, V.
A survey of mobility models for ad hoc network research.
Wireless Communications and Mobile Computing (special issue on mobile ad hoc networking: research, trends and applications), **2** (2002), 483–502.

[34] Boudec, J-Y. L. and Vojnovic, M.
The random trip model: Stability, stationary regime, and perfect simulation. *Ieee/Acm Transactions On Networking*, **14** (6):1153-1166, 2006

[35] Hong, X.
A group mobility model for ad hoc wireless networks.
In *Proceedings of the 2nd ACM International Workshop on Modeling, Analysis and Simulation of Wireless and Mobile Systems* (MSWiM'99), 1999.

Farah Mourad was born in Tripoli, Lebanon, in 1984. She received the diploma degree in electrical engineering from the Lebanese University, Faculty of Engineering, Tripoli, Lebanon, in 2006. She also received the Master degree in systems optimization and safety from the University of Technology of Troyes (UTT), France, in 2007.

Since October 2007, she is a Ph.D. student at the UTT. Her research concerns the localization of mobile sensors and the tracking of targets in mobile sensor networks.

Hichem Snoussi was born in Bizerta, Tunisia, in 1976. He received the diploma degree in electrical engineering from the Ecole Supérieure d'Electricité (Supelec), Gif-sur-Yvette, France, in 2000. He also received the DEA degree and the Ph.D. in signal processing from the University of Paris-Sud, Orsay, France, in 2000 and 2003, respectively. He obtained the HdR from the University of Technology of Compiègne in 2009.

Between 2003 and 2004, he was postdoctoral researcher at IRCCyN, Institut de Recherches en Communications et Cybernétiques de Nantes. He spent short periods as visiting scientist at the Brain Science Institute, RIKEN, Japan and Olin Neuropsychiatry Research Center at the Institute of Living in United States. Between 2005 and 2010, he was an associate professor at the University of Technology of Troyes. Since September 2010, he has been appointed a full professor position at the same university. He is in charge of the regional research program S3 (System Security and Safety) of the CPER 2007–2013 and the CapSec plateform (wireless embedded sensors for security). He is the principal investigator of an ANR-Blanc project (mv-EMD), a CRCA project (new partnership and new technologies) and a GDR-ISIS young researcher project. He is partner of many ANR projects, GIS, strategic UTT programs. He obtained the national doctoral and research supervising award PEDR 2008–2012.

Cédric Richard (S'98—M'01—SM'07) was born January 24, 1970 in Sarrebourg, France. He received the Dipl.-Ing. and the M.S. degrees in 1994 and the Ph.D. degree in 1998 from the University of Technology of Compiègne, France, all in electrical and computer engineering.

From 1999 to 2003, he was an associate professor at the University of Technology of Troyes, France. From 2003 to 2009, he was a full professor at the Institut Charles Delaunay (CNRS FRE 2848) at the UTT, and the supervisor of a group consisting of 60 researchers and Ph.D. In winter 2009 and autumn 2010, he was a visiting researcher with the Department of Electrical Engineering, Federal University of Santa Catarina (UFSC), Florianòpolis, Brazil. Since September 2009, he is a full professor at Fizeau Laboratory (CNRS UMR 6525, Observatoire de la Côte d'Azur), University of Nice Sophia-Antipolis, France. His current research interests include statistical signal processing and machine learning. He is a junior member of the Institut Universitaire de France since Cctober 2010.

Dr. Richard is the author of over 100 papers. He was the General Chair of the XXIth francophone conference GRETSI on Signal and Image Processing that was held in Troyes, France, in 2007, and of the IEEE International Workshop on Statistical Signal Processing that will be held in Nice in 2011. Since 2005, he is a Member of the Board of the Federative CNRS Research Group ISIS on Information, Signal, Images and Vision. He is a Member of GRETSI Association Board and of the EURASIP Society.

He serves as an Associate Editor of the *IEEE Transactions on Signal Processing* since 2006, and of the *EURASIP Signal Processing Magazine* since 2009. In 2009, he was nominated liaison local officer for EURASIP, and member of the Signal Processing Theory and Methods (SPTM) Technical Committee of the IEEE Signal Processing Society. Paul Honeine and Cédric Richard received Best Paper Award for "Solving the pre-image problem in kernel machines: a direct method" at the 2009 IEEE Workshop on Machine Learning for Signal Processing (IEEE MLSP'09).